Dispersion of Cetyltrimethylammonium Bromide (CTAB) Modified Cellulose Nanocrystals in Polypropylene Melt

Xiaoyu Gong , Jonathan Stolz , Yaman Boluk *

Posted Date: 26 June 2023

doi: 10.20944/preprints202306.1786.v1

Keywords: cellulose nanocrystals; polypropylene; dispersion; crystallization; Cetyltrimethylammonium Bromide

Article

Dispersion of Cetyltrimethylammonium Bromide (CTAB) Modified Cellulose Nanocrystals in Polypropylene Melt

Xiaoyu Gong, Jonathan Stolz and Yaman Boluk *

Department of Civil and Environmental Engineering, University of Alberta, Edmonton, AB T6G 2H9, Canada
* Correspondence: yaman.boluk@ualberta.ca

Abstract: This manuscript investigates the dispersion of cetyltrimethylammonium bromide (CTAB) treated cellulose nanocrystals (CNCs) in polypropylene (PP) by melt mixing. FTIR spectra of CTAB-modified CNCs and unmodified CNCs in a PP matrix were used to evaluate the surface treatments. The surface energies and morphologies of CTAB surface modified CNCs in polypropylene (PP) were used to interpret the effects of nanoparticle dispersion on the crystallization and rheological and mechanical properties of the PP matrix.

Keywords: cellulose nanocrystals; polypropylene; dispersion; crystallization; Cetyltrimethylammonium Bromide

1. Introduction

Cellulose is a linear polysaccharide of D-glucose monomers linked by glycosidic bonds that forms crystalline microfibrils and fibers with strong intermolecular hydrogen bonds [1]. Since highly crystalline cellulose is not meltable by heating or soluble in conventional solvents, only its derivatives can be used by melt extrusion or solvent casting. Hence synthetic polymers from petrochemicals eclipsed the utilization of cellulose derivative polymers and plastics. But recently, cellulose has again become an attractive material in the form of cellulose nanocrystals [2]. Cellulose nanocrystals (CNCs) are currently produced in pilot plants by acid hydrolysis of wood pulp. The concentrated (65 %) sulfuric acid hydrolysis process removes the amorphous segments of cellulose fibrils and releases negatively charged cellulose nanocrystal whiskers with sulfate half ester functional groups on surfaces [3]. The highly crystalline CNCs exhibit excellent properties such as nanoscale dimensions (w: 3-10 nm, L: 100-600 nm) [4], high surface area (~250 m^2/g) [5], low density (~1.61g/cm^3) [6], excellent mechanical strength (elastic modulus ~100-200 GPa) [7], and chirality [8].

As a renewable and nontoxic biomaterial, CNCs have attracted tremendous scientific and industrial interest over the past two decades, due to their colloidal, mechanical, and optical properties [7,9]. Therefore, CNCs have been broadly targeted as emerging nanomaterials for applications such as reinforced nanocomposites, biomedicals, optically tunable materials, and emulsion stabilizers [10–14]. CNCs with hydroxyl and half ester sulfate groups are hydrophilic and can be dispersed with relative ease in hydrophilic polymers such as PVA, PEO, starch [15–17] and hydrophobic polymers in aqueous latex suspensions [18,19]. On the other hand, the dispersion of CNCs in nonpolar polymers by using melt mixing is extremely difficult due to CNCs' strong inter-particle interactions. High specific surface area, inter-particle van der Waals interactions and hydrogen bonding result in strong CNCs agglomerates. Hence, it is difficult to disrupt CNCs agglomerates and disperse and distribute them into individual particles within a high viscosity polymer matrix.

Surface modification is a promising technique to enhance CNCs-polymer interactions and disperse them in hydrophobic polymers. CNCs have been extensively modified by chemical treatments, including esterification, etherification, oxidation, and polymer grafting [7]. On the other hand, noncovalent modifications of CNCs, such as the use of surfactants, has attracted considerable attention as a simple route. The negative surface charge of CNCs due to the sulfate-half ester groups

 doi:10.20944/preprints202306.1786.v1

facilitates the adsorption of cationic groups. For instance, cationic cetyltrimethylammonium bromide (CTAB) has been used to produce hydrophobic CNCs [20].

Polypropylene is used as a commodity polymer in various applications due to its good chemical resistance and weldability. It is most widely used in packaging, consumer goods, automotive parts, and medical products. PP-CNCs composites, therefore, generate interest. Successful incorporation of CNCs in PP by melt mixing is investigated by two methods: 1) with a two stage spray-freeze drying of CNCs [21,22]; and 2) by employing poly(ethylene-co-vinyl alcohol) as a melt compatibilizer [23]. It is found that a better dispersion of CNCs in PP matrices results in considerable improvements in mechanical properties and crystallization. Polypropylene is usually converted into finished parts by an injection molding process which runs in cycles. Each cycle comprises filling, packing, and cooling stages. The production rate of a semi-crystalline polymer such as PP into molded parts depends on the cooling (hold) time. Generally nucleation agents are added into PP to increase the rate of crystallization and reduce the cooling time. Hence, if CNCs are dispersed uniformly as individual particles without any aggregates in a polypropylene matrix, they can act as a nucleating agent. This would lead to a rapid decrease in mold pressure due to a rapid crystallization rate of the resin [22,23].

Since a good dispersion of CNCs in PP results in a faster crystallization rate, our objective in this study "was to investigate the dispersion of CTAB modified CNCs in PP by melt mixing. The addition of CNCs can not only increase the nucleation process but also decrease the chain mobility and folding of PP molecules, which have opposite effects on the entire crystallization process. Therefore, we investigated melt mixing of PP only with CNCs at a low concentration (2 wt.%). We described the dispersibility of CTAB surface modified CNCs in a polypropylene (PP) matrix via melt mixing and the effects of dispersion on crystallization, and on rheological and mechanical properties. The hydrophobicity of CNCs was achieved by using cationic surfactant CTAB as a non-covalently bound hydrophobic surface modification agent. Strong electrostatic interactions exist between negatively charged half ester sulfate groups on CNCs and the cationic part of CTAB which will leave the hydrophobic group of CTAB exposed on CNCs surfaces. This technique is preferred over chemical surface modification procedures because it can be used as a "simple" and "in-situ" surface modification method in commercial plants with existing tanks without requiring any capital spending. In this process, CTAB is added into the furnish of a hydrolyzed CNC suspension before the spray drying stage of CNCs manufacturing [24,25]. Since the nucleation and crystallization benefits of uniform dispersion of CNCs have been demonstrated in PP previously [22,23], our focus in this study was to investigate the effects of CTAB treatment of CNCs as a simple, in-situ surface modification technique. To the best of our knowledge, no study has been found in the literature to date on the dispersion of CTAB modified CNCs in PP by melt mixing.

2. Materials and Methods

2.1. Materials

Commercial grade isotactic polypropylene (PP) with a MFR of 12 g/10 min (230^{o}C/2.16 kg) and a melting point of 166^{o}C and cationic surface active agent cetyltrimethylammonium bromide ([($C_{16}H_{33}$)N(CH_3)$_3$]Br (CTAB) were purchased from Sigma Aldrich. PP has the weight average molecular weight (M_w) of 250,000 g/mol and the number average molecular weight (M_n) of 67,000 g/mol. Spray dried CNCs (CNCs) were provided by Innotech Alberta, prepared according to the method previously reported [24].

2.2. Sample Preparation

CTAB modified CNCs were prepared by dispersing CNCs in DI water at 0.5 wt. % and stirred mechanically with an equal volume of 2 mM CTAB solution for 24 hours, followed by a dialysis against deionized water using a crossflow filtration system to remove unbonded CTAB. The drying of CTAB modified CNCs was achieved by applying a single stage of either spray or freeze drying. Freeze and spray drying methods did not show a significant difference in the dispersion of CTAB-

 doi:10.20944/preprints202306.1786.v1

CNCs in PP. Therefore, drying of CTAB treated CNCs was continued only by freeze drying. Untreated hydrophilic CNCs and hydrophobic CTAB modified CNCs are referred to respectively as CNCs and CTAB-CNCs in the text.

A Dynisco Laboratory Mixing Extruder was used for melt mixing of the polymers with CNCs and for extruding filaments. The rotor and header were both set to 190 °C and the drive motor was set to 90 rpm. PP and CNCs were mixed and fed into the extruder's hopper and the extruded samples were collected to form composites with CNC content at 2 wt. %.

2.3. Characterization

PP, CNCs in PP (CNCs-PP), and CTAB-CNCs in PP (CTAB-CNCs-PP) were tested on a Nicole iS 50 FTIR spectrometer (Thermo Fisher Scientific) in attenuated total reflection (ATR) mode. The samples were ground into powder and kept in a vacuum oven at 60 °C for 24 h before the test. All the samples were tested as the average of 64 scans at 4 cm^{-1} resolution and 25 °C.

The morphology of the CNCs-PP and the CTAB-CNCs-PP was characterized by a SEM imaging technique. The samples were coated with gold (3 nm thickness) and visualized on a Hitachi S-4800 Field Emission Gun SEM (Hitachi High-Technologies Canada, Inc. Ontario, Canada).

Wettability and surface free energy analyses of CNCs were performed by measuring the contact angles of the spin coated samples using the contact angle analyzer FTA-200. To calculate the surface energy (γ_s) of the CNCs and CTAB-CNCs, diiodomethane, DI water, and formamide were employed as the droplet liquids. The surface energy parameters of the three liquids are listed elsewhere [26].

Differential scanning calorimetry (DSC) of PP, CNCs-PP, and CTAB-CNCs-PP was performed on a DSC-Q1000 (TA Instruments) under a nitrogen atmosphere. To remove the thermal history, the samples (~ 5 mg) were heated to 220 °C at a constant rate of 50 °C /min and held for 5 min, then cooled to 50 °C at a rate of 80 °C /min. The samples were then heated and cooled following the same protocol in the second cycle. The data in the second cycle was analyzed by TA Universal Analysis software. The crystallinity index (X_c) was calculated from the enthalpy of melting (ΔH_m) using the equation below:

$$X_c = \frac{\Delta H_m}{w_{pp} \times \Delta H_m^0} \quad (1)$$

where w_{pp} is the weight fraction of the PP phase and ΔH_m^0 is the enthalpy of the 100% crystalline PP (207 J/g) [27].

The rheological properties of the molten polymer were tested with a TA Instruments AR-G2 rheometer. Tests were performed at 200°C in the rheometer's furnace with a 25 mm diameter parallel plate geometry. Frequency sweep tests were performed from 0.1 to 500 rad/s at a strain amplitude of 1%, which had been found to be within the linear viscoelastic range for all the polymer and polymer composite melts.

The dynamic mechanical properties of the polymer were tested with a TA Instruments Q800 Dynamic Mechanical Analyzer (DMA). A piece of polymer fiber roughly 1 mm in diameter by 20 mm in length was mounted in the DMA and tested in tension. Displacement was applied in a sinusoidal pattern with a strain amplitude of 0.1% and a frequency of 1 Hz. The force applied was measured and used by the system to calculate the viscoelastic properties of the material. This test was applied over a temperature range of 25°C to 100°C.

3. Results and discussion

3.1. Adsorption of CTAB molecules on CNCs

The adsorption of positively charged CTAB onto the negatively charged CNCs has been investigated and will be published in another study, in which the surface properties of CNCs have been tailored by various amounts of CTAB (0.25-32 mM). In the current study, the CTAB-CNCs prepared by 2 mM CTAB was used for all the CTAB-CNCs-PP. To study the molecular interaction between CTAB-CNCs and PP, FTIR spectra of pure PP, CNCs-PP, and CTAB-CNCs-PP were

 doi:10.20944/preprints202306.1786.v1

recorded. As shown in Figure 1, PP showed -C-H stretching vibrations in the range of 2830-2950 cm^{-1} and C-H bending vibrations at 1375 and 1456 cm^{-1} [28]. Compared to the spectrum of PP, the characteristic absorbance of CNCs-PP did not change significantly except that the peak strength decreased which was due to the introduction of CNCs into the PP matrix. The absorbance of CNCs was not observed due to the low content of CNCs in PP and the weak characteristic peaks of CNCs have been overlapped by the absorbance of PP. However, compared to the spectra of PP and CNCs-PP, the characteristic absorbance in the range of 2830-2950 cm^{-1} and at 1375 and 1456 cm^{-1} further decreased. More importantly, characteristic absorbances at 3340 cm^{-1} (-OH stretching) and 1480 cm^{-1} (symmetric vibration of the head group N^+-CH_3 in CTAB-CNCs) appeared in the spectrum of CTAB-CNCs-PP, indicating that CTAB treated CNCs had been successfully incorporated into the PP matrix [29,30]

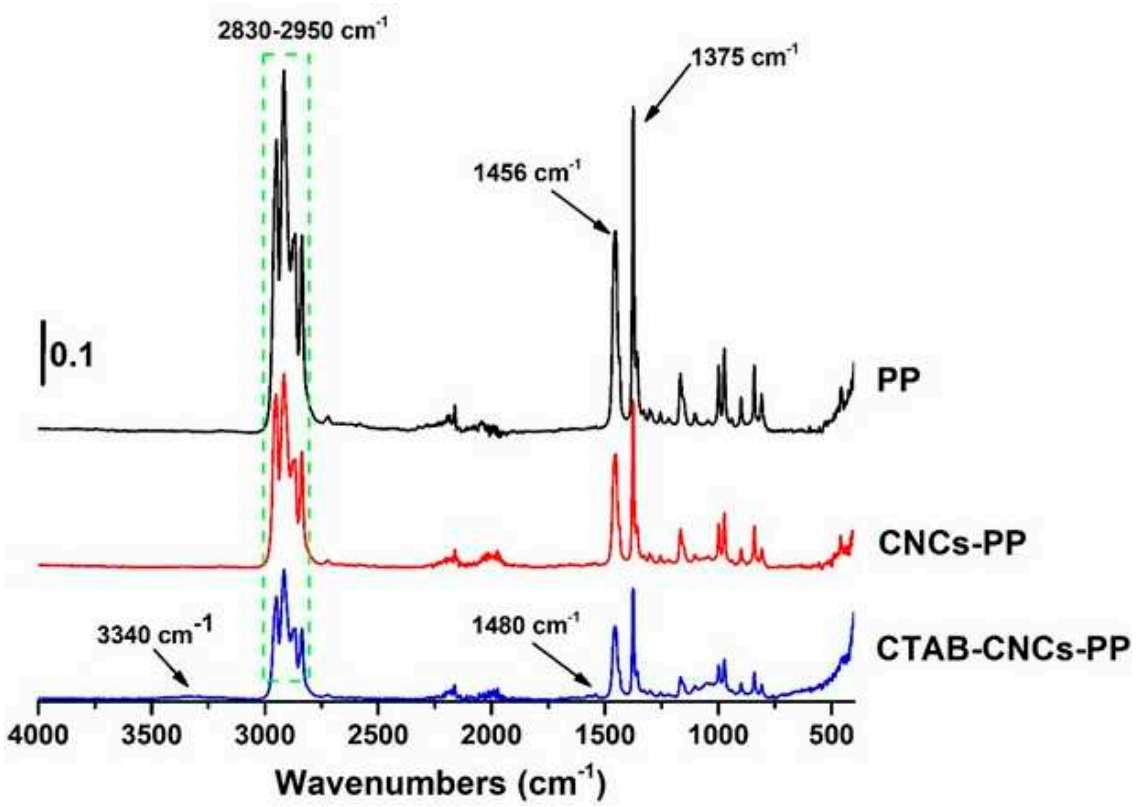

Figure 1. The FTIR spectra of PP, CNCs-PP, and CTAB-CNCs-PP.

3.2. Analysis of Dispersion

Figure 2 shows the morphology of the CNCs-PP composite and the CTAB-CNCs-PP composite. The CNCs-PP composite exhibited a coarse surface with a great number of aggregates. The aggregates were categorized into two main portions, in which the relatively larger aggregates randomly embedded in the matrix had a dimension scale of around 100 μm, while the more randomly distributed aggregates of smaller size were observed with increased magnification. These aggregates were attributed to poorly mixed CNCs, as a clear filler-matrix structure was presented in the composite. Nevertheless, the CTAB-CNCs-PP composite exhibited a different morphology, with a relatively smoother surface and fewer large aggregates. Indeed, smaller aggregates were dominant in the CTAB-CNCs-PP composite, indicating a better dispersion of CTAB-CNCs in the PP matrix when compared with the dispersion of CNCs in the PP matrix. CNCs are regarded as highly hydrophilic materials due to the abundant hydroxyl groups on their surfaces. The dispersion of CNCs in PP was significantly improved after CTAB modification as the long alkyl chains of CTAB attached to the surface of CNCs forming a hydrophobic layer that facilitated the dispersion of CNCs in the hydrophobic PP matrix.

Preprints (www.preprints.org) | NOT PEER-REVIEWED | Posted: 26 June 2023 doi:10.20944/preprints202306.1786.v1

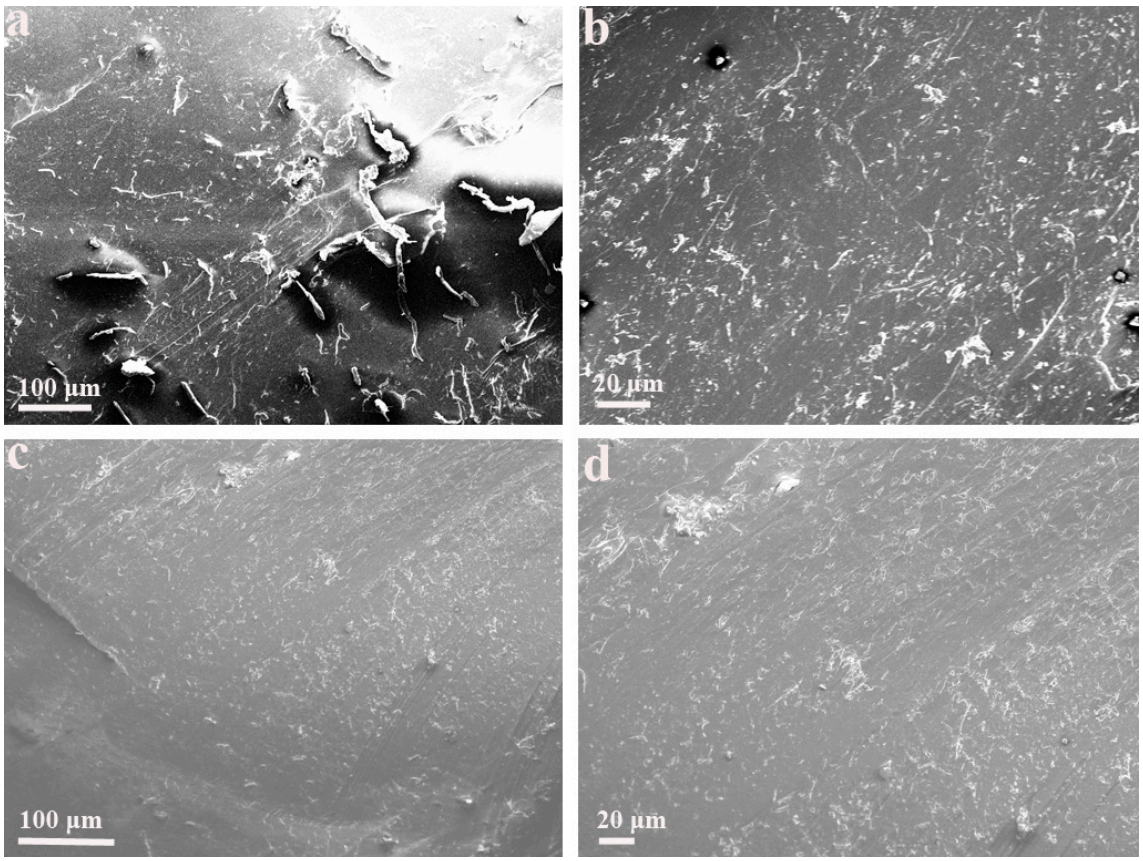

Figure 2. SEM images of CNCs-PP (a and b) and CTAB-CNCs-PP composite (c and d).

The polar and dispersive components of surface energy ($\gamma_p$and γ_d) and the total surface energy (γ_s) of CNCs and CTAB-CNCs were calculated from contact angle data by following the van Oss-Chaudry-Good theory (vOCG theory) [31] and presented along with PP data (Table 1). The polar component of CNCs decreased from 31.34 mJ/m² to 16.16 mJ/m², while the total surface energy decreased from 70.76 mJ/m² to 50.38 mJ/m² after the CTAB modification, indicating that the surface modification had significantly decreased the polarity of CNCs molecules. Khoshkava and Kamal have calculated the total surface energy of PP to be 32.1 mJ/m² of which the polar component of PP is 0.5 mJ/m². Surface energy data demonstrated that the CTAB modification significantly increased the hydrophobicity of CNCs and facilitated dispersion of CTAB-CNCs in the PP matrix.

Table 1. Contact angles and surface energy components of PP, CNCs and CTAB-CNCs.

Material	θ_{Water}	$\theta_{Formamide}$	$\theta_{Diiodomethane}$	γ_d (mJ/m²)	γ_p (mJ/m²)	γ_s (mJ/m²)
PP [32]	98±2.3	79±0.8*	57±0.8	31.6	0.5	32.1
CNCs	16±2.0	11±2	22±3	39.42	31.34	70.76
CTAB-CNCs	56±1.5	38±2	45±1	34.22	16.16	50.38

* Glycerol

3.3. DSC Properties

The melting point (T_m), enthalpy of melting (ΔH_m), onset temperature of crystallization (T_c), and crystallinity index (X_c) of PP, CNCs-PP, and CTAB-CNCs-PP are presented in Table 2. With the addition of CNCs, the melting point and onset temperature of crystallization of PP did not change too much, whereas the addition of the CTAB-CNCs into the PP matrix increased the T_m from 169.02 to 174.11°C and T_c from 111.71 to 116.95°C. The presence of well-dispersed CTAB-CNCs in PP acts as

Preprints (www.preprints.org) | NOT PEER-REVIEWED | Posted: 26 June 2023 doi:10.20944/preprints202306.1786.v1

a nucleating agent which decreases the activation energy and the rate of nucleation, because the formation of a heterogeneous nucleus is more favorable on a heterogeneous surface than in the bulk PP melts. Consequently, significantly more nuclei are formed in the presence of CTAB-CNCS. More perfect lamellas were expected to be formed during the crystallization because crystallization shifted to a higher temperature. The higher the T_c value means a more rapid crystallization process which requires a shorter cycle time in injection molding.

Table 2. Melting point (T_m), enthalpy of melting (ΔH_m), the onset temperature of crystallization (T_c), and crystallinity index (X_c) of PP, CNCs-PP, and CTAB-CNCs-PP.

Samples	T_m (°C)	ΔH_m (J/g)	T_c (°C)	X_c
PP	169.02	95.80	111.71	0.47
CNCs-PP	168.02	99.86	112.05	0.49
CTAB-CNCs-PP	174.11	102.10	116.95	0.50

It was noted that the X_c slightly increased after the addition of CNCs or CTAB-CNCs into the PP matrix. The total amount of nuclei and the mobility of polymers both affect the total crystallinity of the polymer-nanoparticle system [27]. With the addition of nanocrystals into PP matrix, the total amount of nuclei increased while the mobility of matrix molecules decreased. In this study, even though the weight fraction of unmodified CNCs and CTAB-CNCs in PP composites was kept at 2%, the mobility of PP molecules was significantly influenced by the molecular interactions between PP and CNCs or PP and CTAB-CNCs. Due to the poor dispersion of CNCs in the PP matrix, the hydrophilic CNCs could hardly interact with the hydrophobic PP matrix, resulting in large aggregates and phase separation of CNCs as observed from SEM images. Therefore, unmodified CNCs did not exhibit a significant influence on the thermal property and crystallization behavior of the PP. However, hydrophobic CTAB-CNCs could interact with the PP matrix and work as a nucleating agent for the crystallization of PP molecules, and in the meantime could significantly decrease the mobility of PP molecules due to the hydrophobic interaction between PP and CTAB-CNCs.

3.4. Rheological Properties

Figure 3 shows the complex viscosity and storage modulus vs angular frequency of unfilled PP, CNCs-PP, and CTAB-CNCs-PP melts measured at 200 °C. All of the samples exhibited frequency dependent complex viscosities in which the complex viscosity reached a plateau at low frequencies and exhibited a linear decrease on a log-log plot at higher frequencies. Since it is only possible to measure viscosities at high frequencies rather than at high shear rates in a parallel plate rheometer, all of the rheological measurements of melt samples were carried out in linear deformation instead of at a steady state shear flow. Nevertheless, a simple relationship called the "Cox-Merz rule" [33] exists between linear and nonlinear viscoelastic properties, polymer melts and solutions by overlapping the steady-state shear viscosity, $\eta(\dot{\gamma})$ with the magnitude of complex viscosity, $|\eta^*|(\omega)$ while $\dot{\gamma} = \omega$. Therefore, steady shear viscosities of melt samples were discussed in place of measured complex viscosities. All the samples exhibited non-Newtonian viscosities, in which viscosity reached a plateau at low shear rates and shear thinning at high shear rates. Since only a small amount (wt. 2%) of CNCs and CTAB-CNCs were melt mixed in PP, they did not significantly affect the viscosity and its shear rate behavior. Therefore, the addition of 2% CNCs and CTAB-CNCs is not expected to interfere with the melt flow during the filling and packing stages of the injection molding cycles.

Preprints (www.preprints.org) | NOT PEER-REVIEWED | Posted: 26 June 2023 doi:10.20944/preprints202306.1786.v1

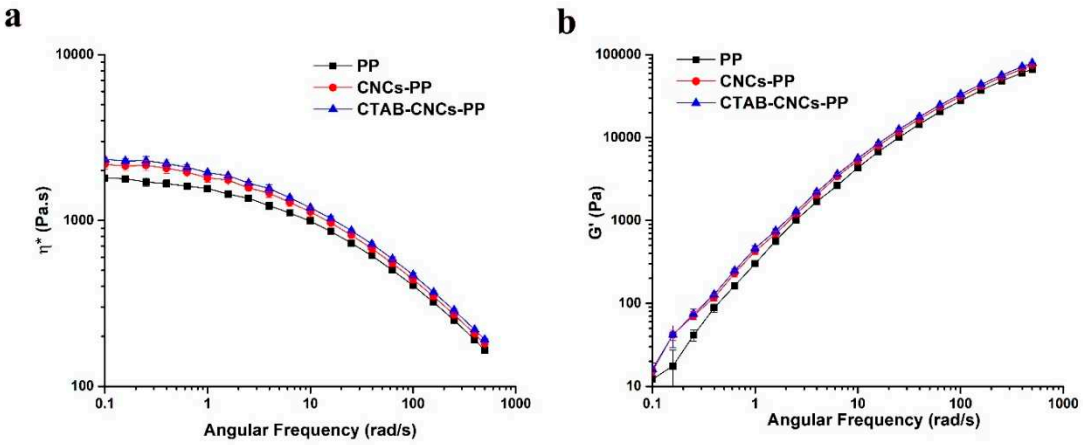

Figure 3. Complex viscosity (a) and storage modulus (b) of PP, CNCs-PP, and CTAB-CNCs-PP.

Despite the small changes, the complex viscosity and the storage modulus of the three molten samples followed a sequence of CTAB-CNCs-PP melt > CNCs-PP melt > PP melt for all of the frequency ranges. Among the three melt samples, CTAB-CNCs showed the highest complex viscosity and storage modulus, which was due to the better dispersion of CTAB-CNCs in the PP matrix and the stronger adhesion between CTAB-CNCs and PP molecules when compared with that of unmodified CNCs in the PP matrix. The interfacial tension between PP and CTAB-CNCs decreased with the hydrophobicity level of CTAB-CNCs as shown with surface energies in Table 1. CTAB surface modification lowered the polarity of CNCs, decreased the interfacial tension for CTAB-CNCs-PP and the barrier energy, and therefore increased the dispersion of CTAB-CNCs in PP.

3.5. Dynamic Mechanical Properties

The dynamic mechanical properties are critically important for evaluating the performance of polymer composites. Figure 4 shows the evolution of storage modulus (E′) and tan (δ) of 2 wt.% CNCs in PP and CTAB-CNCs in PP nanocomposites along with PP as a function of temperature ranging from 25 °C to 100 °C. The storage modulus of the samples decreased with the increase in temperature, which was mainly due to the decrease in stiffness of the PP matrix [34]. It was noted the storage modulus of CTAB-CNCs-PP was higher than that of CNCs-PP which was higher than that of the unfilled PP, indicating that the addition of fillers (CTAB-CNCs and CNCs) could increase the stiffness of the PP matrix, as nanofillers reinforce the storage modulus (E′) of the PP composite by restricting the motion of PP molecule chains [35]. In the current study, CNCs and CTAB-CNCs enhanced the mechanical properties of the PP matrix via the formation of a rigid percolating filler network that was cemented together by hydrogen bonds [7]. When compared with the CNCs-PP nanocomposite, the CTAB-CNCs-PP nanocomposite showed a higher storage modulus (E′) throughout the whole temperature range, suggesting that the CTAB modification enhanced the mechanical property of the nanocomposite. This could be due to the better dispersion of CTAB-CNCs in the PP matrix, the stronger adhesion between CTAB-CNCs and PP molecules and the better crystallization of PP when compared with that of CNCs in the PP matrix. As shown in the SEM images, CNCs tended to form larger aggregates in the PP matrix, while the CTAB-CNCs formed into relatively smaller aggregates and had better dispersion in the PP matrix. Additionally, due to the hydrophobic layer of the long alkyl chains of CTAB on the surface of CTAB-CNCs, the hydrophobic interaction between CTAB-CNCs and PP was stronger. Nevertheless, due to the low concentration of CTAB-CNCs (2 wt.%) the increase in the storage modulus was only 20% compared to unfilled PP.

Preprints (www.preprints.org) | NOT PEER-REVIEWED | Posted: 26 June 2023 doi:10.20944/preprints202306.1786.v1

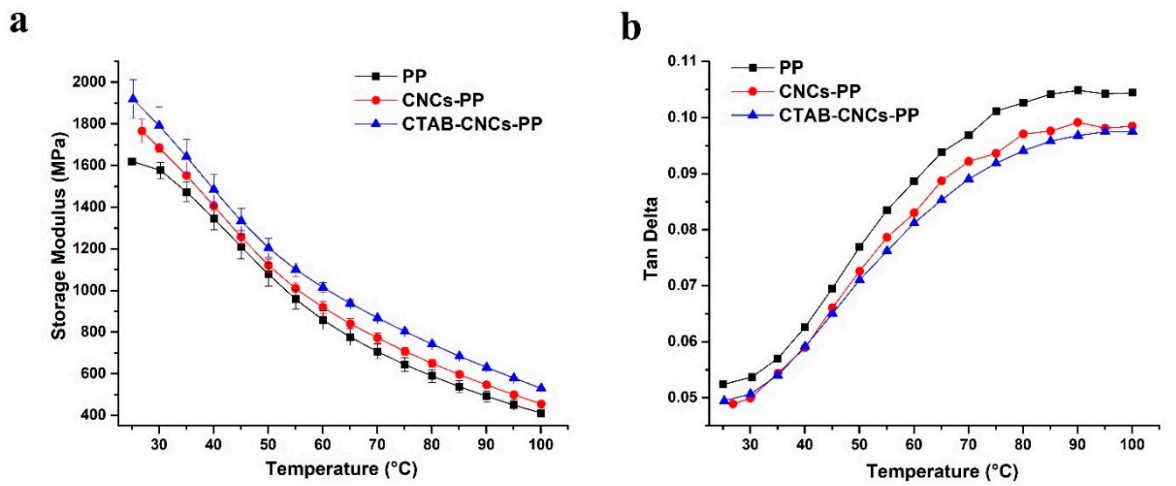

Figure 4. Storage modulus (a) and tan delta (b) of PP, CNCs-PP, and CTAB-CNCs-PP.

Moreover, the tan (δ) of all the PP-based materials was lower than 0.11, indicating that all samples had a solid-like structure during temperatures ranging between 25 °C to 100 °C, as PP has a glass transition temperature between -20 °C to 20 °C and a melting temperature of around 160 °C [34]. Overall, the tan (δ) value of the three samples followed a sequence of PP > CNCs-PP nanocomposite > CTAB-CNCs-PP nanocomposite over the entire temperature range, which was due to the reinforcement effect of the two nanofillers in the PP matrix that stiffened the nanocomposite. More interestingly, the tan (δ) value of the three samples at lower temperatures (25 °C to 60 °C) was relatively close, with the curve of CTAB-CNCs-PP almost superimposing over that of the CNCs-PP nanocomposite. However, the three curves separate increasingly at higher temperature (60 °C to 100 °C), and the previously superimposed CTAB-CNCs-PP and CNCs-PP curves part from each other, indicating that the structure of the CTAB-CNCs-PP nanocomposite is relatively stable at higher temperatures, which is also due to the better dispersion of CTAB-CNCs in the PP matrix and the stronger adhesion between CTAB-CNCs and PP molecules when compared with that of CNCs in the PP matrix.

4. Conclusion

The surface properties of CNCs were modified with a simple CTAB treatment and a better dispersion in PP was obtained by melt processing. Morphological observation indicates that CTAB modification decreased the polar component of the surface energy of CNCs and significantly improved its dispersion in the PP matrix. The DSC study showed that CTAB-CNCs in PP increased T_c which means a more rapid crystallization process and a shorter cycle time in injection molding.

The addition of CNCs and CTAB-CNCs in PP at 2.0 % concentration slightly increased complex viscosity and the storage modulus of the PP melts. The increase was slightly higher in CTAB-CNCs-PP than CNCs-PP melts due to a better dispersion of cellulose nanocrystals. Nevertheless, those increases were not significant and the addition of CNCs and CTAB-CNCs is not expected to interfere with the melt flow during the filling and packing stages of the injection molding cycles.

Better dispersion of CTAB-CNCs in the PP matrix and a stronger adhesion between CTAB-CNCs and PP molecules when compared with that of CNCs in the PP matrix resulted in a higher storage modulus (E′). The elastic modulus of CTAB-CNCs-PP was 20% higher than PP and 10% higher than unmodified CNCs-PP. The tan (δ) value of the three samples followed a sequence of PP > CNCs-PP nanocomposite > CTAB-CNCs-PP nanocomposite over the entire temperature range, which was due to the reinforcement effect of the two nanofillers in the PP matrix that stiffened the nanocomposite.

CRediT authorship contribution statement: Xiaoyu Gong: Methodology, Formal analysis, Investigation, Data curation, Writing-original draft, Writing-review & editing, Visualization. Jonathan Stolz: Methodology, Formal

analysis, Investigation, Data curation, Writing-original draft, Visualization. Yaman Boluk: Conceptualization, Methodology, Writing-review & editing, Supervision, Funding acquisition.

Acknowledgement: We greatly acknowledge the funding support of Alberta Innovates, Alberta Bio Future (ABF) Biomaterials Pursuit Program for funding the project BFR006. We thank InnoTech Alberta for the generous supply of cellulose nanocrystals.

Declaration of competing interest: The authors declare that they have no known competing financial interests or personal relationships that could have appeared to influence the work reported in the communication.

References

1. D. Klemm, B. Heublein, H.P. Fink, A. Bohn, Cellulose: fascinating biopolymer and sustainable raw material, Angewandte chemie international edition, 44 (2005) 3358-3393.
2. M.S. Reid, M. Villalobos, E.D. Cranston, Benchmarking cellulose nanocrystals: from the laboratory to industrial production, Langmuir, 33 (2017) 1583-1598.
3. W.Y. Hamad, T.Q. Hu, Structure–process–yield interrelations in nanocrystalline cellulose extraction, The Canadian Journal of Chemical Engineering, 88 (2010) 392-402.
4. R.R. Lahiji, Y. Boluk, M. McDermott, Adhesive surface interactions of cellulose nanocrystals from different sources, Journal of Materials Science, 47 (2012) 3961-3970.
5. N. Grishkewich, N. Mohammed, J. Tang, K.C. Tam, Recent advances in the application of cellulose nanocrystals, Current Opinion in Colloid & Interface Science, 29 (2017) 32-45.
6. S. Elanthikkal, T. Francis, C. Sangeetha, G. Unnikrishnan, Cellulose whisker-based green polymer composites, Handbook of Composites from Renewable Materials, ed. VK Thakur, MK Thakur, and MR Kessler. Wiley, USA, (2017) 461-494.
7. Y. Habibi, L.A. Lucia, O.J. Rojas, Cellulose Nanocrystals: Chemistry, Self-Assembly, and Applications, Chem. Rev., 110 (2010) 3479-3500.
8. K.E. Shopsowitz, H. Qi, W.Y. Hamad, M.J. MacLachlan, Free-standing mesoporous silica films with tunable chiral nematic structures, Nature, 468 (2010) 422-425.
9. D. Trache, M.H. Hussin, M.M. Haafiz, V.K. Thakur, Recent progress in cellulose nanocrystals: sources and production, Nanoscale, 9 (2017) 1763-1786.
10. N. Lin, J. Huang, A. Dufresne, Preparation, properties and applications of polysaccharide nanocrystals in advanced functional nanomaterials: a review, Nanoscale, 4 (2012) 3274-3294.
11. R. Sunasee, U.D. Hemraz, K. Ckless, Cellulose nanocrystals: a versatile nanoplatform for emerging biomedical applications, Expert opinion on drug delivery, 13 (2016) 1243-1256.
12. M. Roman, D.G. Gray, Parabolic focal conics in self-assembled solid films of cellulose nanocrystals, Langmuir, 21 (2005) 5555-5561.
13. I. Capron, B. Cathala, Surfactant-free high internal phase emulsions stabilized by cellulose nanocrystals, Biomacromolecules, 14 (2013) 291-296.
14. X. Gong, T. Liu, H. Zhang, Y. Liu, Y. Boluk, Release of Cellulose Nanocrystal Particles from Natural Rubber Latex Composites into Immersed Aqueous Media, ACS Applied Bio Materials.
15. Z. Jahan, M.B.K. Niazi, Ø.W. Gregersen, Mechanical, thermal and swelling properties of cellulose nanocrystals/PVA nanocomposites membranes, Journal of industrial and engineering chemistry, 57 (2018) 113-124.
16. O.V. Surov, M.I. Voronova, A.V. Afineevskii, A.G. Zakharov, Polyethylene oxide films reinforced by cellulose nanocrystals: Microstructure-properties relationship, Carbohydrate polymers, 181 (2018) 489-498.
17. V. Nessi, X. Falourd, J.-E. Maigret, K. Cahier, A. D'orlando, N. Descamps, V. Gaucher, C. Chevigny, D. Lourdin, Cellulose nanocrystals-starch nanocomposites produced by extrusion: Structure and behavior in physiological conditions, Carbohydrate polymers, 225 (2019) 115123.
18. G. Siqueira, H. Abdillahi, J. Bras, A. Dufresne, High reinforcing capability cellulose nanocrystals extracted from Syngonanthus nitens (Capim Dourado), Cellulose, 17 (2010) 289-298.
19. X. Gong, T. Liu, H. Zhang, Y. Liu, Y. Boluk, Release of Cellulose Nanocrystal Particles from Natural Rubber Latex Composites into Immersed Aqueous Media, ACS Applied Bio Materials, 4 (2021) 1413-1423.
20. C. Brinatti, J. Huang, R.M. Berry, K.C. Tam, W. Loh, Structural and energetic studies on the interaction of cationic surfactants and cellulose nanocrystals, Langmuir, 32 (2016) 689-698.
21. V. Khoshkava, M.R. Kamal, Effect of cellulose nanocrystals (CNC) particle morphology on dispersion and rheological and mechanical properties of polypropylene/CNC nanocomposites, ACS applied materials & interfaces, 6 (2014) 8146-8157.
22. V. Khoshkava, H. Ghasemi, M.R. Kamal, Effect of cellulose nanocrystals (CNC) on isothermal crystallization kinetics of polypropylene, Thermochimica Acta, 608 (2015) 30-39.

23. D. Bagheriasl, P. Carreau, C. Dubois, B. Riedl, Properties of polypropylene and polypropylene/poly (ethylene-co-vinyl alcohol) blend/CNC nanocomposites, Composites Science and Technology, 117 (2015) 357-363.
24. Y. Esparza, T.-D. Ngo, C. Fraschini, Y. Boluk, Aggregate Morphology and Aqueous Dispersibility of Spray-Dried Powders of Cellulose Nanocrystals, Industrial & Engineering Chemistry Research, 58 (2019) 19926-19936.
25. Y. Esparza, T.-D. Ngo, C. Fraschini, Y. Boluk, Effects of additives on the particle morphology and aqueous dispersibility of foam-spray dried cellulose nanocrystal suspensions, Cellulose, 26 (2019) 8611-8623.
26. X. Gong, M. Kalantari, S. Aslanzadeh, Y. Boluk, Interfacial interactions and electrospinning of cellulose nanocrystals dispersions in polymer solutions: a review, Journal of Dispersion Science and Technology, (2020) 1-59.
27. D. Bagheriasl, P.J. Carreau, C. Dubois, B. Riedl, Properties of polypropylene and polypropylene/poly(ethylene-co-vinyl alcohol) blend/CNC nanocomposites, Composites Science And Technology, 117 (2015) 357-363.
28. J. d'Eon, W. Zhang, L. Chen, R.M. Berry, B.X. Zhao, Coating cellulose nanocrystals on polypropylene and its film adhesion and mechanical properties, Cellulose, 24 (2017) 1877-1888.
29. W.T. Li, F. Xiao, H. Su, D.S. Wang, X.F. Yang, Investigation of adsorption and photocatalytic activities of in situ cetyltrimethylammonium bromide-modified Bi/BiOCl heterojunction photocatalyst for organic contaminants removal, Rsc Advances, 6 (2016) 93309-93317.
30. T. Abitbol, H. Marway, E.D. Cranston, Surface modification of cellulose nanocrystals with cetyltrimethylammonium bromide, Nordic Pulp & Paper Research Journal, 29 (2014) 46-57.
31. C. Van Oss, R. Good, M. Chaudhury, Additive and nonadditive surface tension components and the interpretation of contact angles, Langmuir, 4 (1988) 884-891.
32. V. Khoshkava, M. Kamal, Effect of surface energy on dispersion and mechanical properties of polymer/nanocrystalline cellulose nanocomposites, Biomacromolecules, 14 (2013) 3155-3163.
33. R.B. Bird, R.C. Armstrong, O. Hassager, Dynamics of polymeric liquids. Vol. 1: Fluid mechanics, (1987).
34. M. Cordin, T. Bechtold, T. Pham, Effect of fibre orientation on the mechanical properties of polypropylene-lyocell composites, Cellulose, 25 (2018) 7197-7210.
35. A.N. Gaduan, L. Solhi, E. Kontturi, K.Y. Lee, From micro to nano: polypropylene composites reinforced with TEMPO-oxidised cellulose of different fibre widths, Cellulose, 28 (2021) 2947-2963.